The proliferation of human mucosal-associated invariant T cells requires a MYC-SLC7A5-glycolysis metabolic axis

Kedia-Mehta, Nidhi; Pisarska, Marta M; Rollings, Christina; O'Neill, Chloe; De Barra, Conor; Foley, Cathriona; Wood, Nicole A W; Wrigley-Kelly, Neil; Veerapen, Natacha; Besra, Gurdyal; Bergin, Ronan; Jones, Nicholas; O'Shea, Donal; Sinclair, Linda V; Hogan, Andrew E

DOI:
10.1126/scisignal.abo2709

Editor's summary:

The master regulator of innate T cell metabolism

Mucosal associated invariant T (MAIT) cells are a type of innate-like T cells that are enriched in adipose, gut, and liver tissue and that recognize bacterial metabolites. Upon activation, they proliferate and produce cytokines to promote host defense. Kedia-Mehta et al. showed that MAIT proliferation depended on MYC-associated pathways involving amino acid transport and glycolysis. Furthermore, MAIT cells from patients with obesity showed disrupted function and engagement of these pathways. These findings demonstrate that the canonical metabolic pathways found in conventional T cells are active in MAIT cells and may be relevant to the development of MAIT cell-based therapies and the study of obesity. -AEB

The proliferation of human mucosal associated invariant T cells requires a MYC-SLC7A5-glycolysis metabolic axis

Nidhi Kedia-Mehta[1*], Marta M. Pisarska[1,2*], Christina Rollings[3], Chloe O'Neill[2], Conor De Barra[2], Cathriona Foley[4], Nicole AW. Wood[1,2], Neil Wrigley-Kelly[5], Natacha Veerapen[6], Gurdyal Besra[6], Ronan Bergin[2], Nicholas Jones[7], Donal O'Shea[2,5], Linda V. Sinclair[3#] and Andrew E. Hogan[1,2#]

Affiliations: [1.]Kathleen Lonsdale Institute for Human Health Research, Maynooth University, Maynooth, Co Kildare. Ireland. [2.]National Children's Research Centre, Dublin 12, Ireland. [3.] Division of Cell Signaling and Immunology, School of Life Sciences, University of Dundee, United Kingdom. [4.]Department of Biological Sciences, Munster Technological University, Cork, Ireland. [5.] St Vincent's University Hospital & University College Dublin, Dublin 4, Ireland. [6.] School of Biosciences, University of Birmingham, United Kingdom. 7. Institute of Life Science, Swansea University Medical School, Swansea, United Kingdom.

*These authors contributed equally to this study.
[#]Joint Senior Authors.

Address for correspondence:
Dr Andrew E. Hogan –
Email: Andrew.E.Hogan@mu.ie

Dr Linda V. Sinclair -
Email: L.V.Sinclair@dundee.ac.uk

Running title: MYC controls MAIT cell proliferation

Keywords: Mucosal associated invariant T cells, Metabolism, MYC, Proliferation, Obesity

Abstract

Mucosal associated invariant T (MAIT) cells are an abundant population of innate T cells that recognize bacterial ligands and play a key role in host protection against bacterial and viral pathogens. Upon activation, MAIT cells undergo proliferative expansion and increase their production of effector molecules such as cytokines. In this study, we found that mRNA and protein the abundance of the key metabolism regulator and transcription factor MYC was increased in stimulated MAIT cells. Using quantitative mass spectrometry, we identified the activation of two MYC controlled metabolic pathways, amino acid transport and glycolysis, both of which were necessary for MAIT cell proliferation. Finally, we showed that MAIT cells isolated from people with obesity showed decreased *MYC* mRNA abundance upon activation, which was associated with defective MAIT cell proliferation and functional responses. Collectively, our data uncovers the importance of MYC-regulated metabolism for MAIT cell proliferation and provides additional insight into the molecular basis for the functional defects of MAIT cells in obesity.

Introduction

Mucosal Associated Invariant T (MAIT) cells are a population of non-MHC restricted T cells that are important in the immune defence against bacterial and viral infections[1, 2, 3, 4, 5]. In addition to their abundance (2-10% of total T cells) in peripheral blood, MAIT cells are relatively abundant across of range of human tissues including adipose, gut and the liver where they can account for up to 50% of all T cells[6]. MAIT cells are early responding T cells that are capable of producing multiple cytokines rapidly upon activation such as IFN-γ, TNF and IL-17[1, 7]. Due to their robust production of effector molecules, MAIT cells have been implicated in both host protection (against pathogens[6] and cancer cells[8]) and tissue repair[9, 10, 11]. MAIT cells are activated when their invariant T cell receptor (TCR) recognise bacterial derivatives presented on the MHC-like molecule MR1[5, 7]. MAIT cells can also be activated in a T cell receptor-independent manner, through cytokine stimulation[10, 12]. Altered MAIT cell cytokine profiles have been reported in several diseases including obesity, arthritis, and viral infection[13, 14, 15, 16, 17, 18].

One key functional response of MAIT cells is their ability to proliferate rapidly upon activation, which has been demonstrated both in vitro and in vivo[19, 20, 21]. Increased immune signal-driven proliferation relies upon metabolic reprogramming to provide the large amounts of energy and biosynthetic intermediates needed to support the rapid generation of new cells[22]. In conventional T cells, metabolic reprogramming in response to activation is controlled by the transcription factor MYC, which acts as a master metabolic regulator[23]. MYC expression is rapidly induced after T cell receptor (TCR) stimulation, and is sustained by amino acid availability and Interleukin 2 (IL-2) signalling[24, 25,26]. In particular, the expression of the amino acid transporter SLC7A5, which is under the control of MYC, forms a forward feeding loop in which amino acid transport through SLC7A5 sustains MYC protein expression[24]. Whether MYC acts as a metabolic regulator in MAIT cells is currently unknown. Although it is known that MAIT cell cytokine production is dependent on glycolytic metabolism, it is unclear what regulates and fuels MAIT cell proliferation[27]. To address these unknowns, we have interrogated the molecular and metabolic requirements for MAIT cell proliferation. In addition, defective Natural Killer (NK) and MAIT cell metabolism and defective cellular

responses are present in people with obesity, which may translate to elevated incidences of co-morbid diseases[27, 28, 29]. However, the impact of obesity on important metabolic regulators such as MYC are not clearly understood and remain to be elucidated.

Using quantitative mass spectrometry, we identified a robust upregulation of MYC expression and MYC controlled metabolic pathways in stimulated MAIT cells. We showed that MYC-regulated metabolic pathways (including amino acid transport and glycolysis) are essential for human MAIT cell proliferation. Finally, we showed that obesity is associated with defective MAIT cell proliferation, due to a defective MYC-SLC7A5-Glycolysis metabolic axis. Collectively, our data demonstrated that MYC acts as a metabolic regulator in TCR and cytokine stimulated MAIT cells and that this is essential for proliferation, and provides further molecular insight into obesity related defects in human MAIT cells.

RESULTS

MAIT cells remodel their proteomes upon TCR activation.

To investigate the major pathways regulating MAIT cell activation, we performed quantitative mass spectrometry on MAIT cells expanded by treatment with IL-2 ($MAIT^{IL\text{-}2}$ cells) before and after TCR stimulation (anti-TCR/CD28 and IL-12/IL-18; $MAIT^{STIM}$). We identified 5740 proteins in both IL-2 maintained and stimulated MAIT cells and have estimated the absolute protein copy number per cell using the proteomic ruler method which uses the mass spectrometry signal of histones as an internal standard[30] (Supplementary File 1). Only a small proportion of highly abundant proteins account for the majority of cellular mass in conventional effector T cells[24, 31, 32]; in human MAIT cells, we found that expression of 8 proteins (Supplementary Figure 1) contribute 25% of the total mass, and expression abundance of approximately 350 proteins accounts for 75 % of the total cellular mass (Figure 1A) Upon TCR activation, we observed remodelling of the $MAIT^{IL\text{-}2}$ cell proteome (Figure 1B), which was accompanied by an increase in total protein mass and cell size (Figure 1C-D). The expression of the most abundant proteins did not change after stimulation and remained proportional to the amounts expressed basally in $MAIT^{IL\text{-}2}$ cells

(Supplementary Figure 1). Signature effector proteins such as Interferon gamma (IFNG) and Granzyme B (GRZB) were amongst the most highly increased proteins upon stimulation (Figure 1E-F). We were also able to detect many proteins associated with a core MAIT cell signature; including IL-18R1 (which strongly increased expression in response to stimulation), KLRB1 (moderate increase), DPPIV (moderately decreased), and TRAV1-2 (expression is decreased upon stimulation) (Figure 1E). In total, 780 proteins were increased more than 1.5-fold upon activation (Figure 1B&F). Pathway analysis highlighted that the increased proteins were enriched in multiple processes and included a large proportion involved in governing cellular metabolism (Figure 1G).

MAIT cells upregulate expression of the transcription factor MYC and its downstream target pathways upon activation.

In silico pathway analysis of a previously published RNA sequencing data-set [10] revealed that MAIT cells activated ex vivo ($MAIT^{EX\text{-}VIVO}$ cells) have a strong MYC signature as determined by the Hallmark gene set enrichment analysis (Figure 2A & Supplementary Figure 2). In our activated human $MAIT^{IL\text{-}2}$ proteomic dataset, we also found increased MYC expression and its target proteins (Figure 2B-C). Using alternative methods to measure MYC expression, we show MYC protein expression is increased in $MAIT^{IL2}$ stimulated through their TCR (Figure 2D-E). We next interrogated MYC expression in TCR stimulated $MAIT^{EXVIVO}$ cells (Figure 2F-G). Together these data show MYC is increased in response to TCR stimulation in both $MAIT^{EX\ VIVO}$ and $MAIT^{IL2}$ expanded cells. To further support the increased expression of MYC targets in activated MAIT cells, we analyzed another published RNA sequencing data set[11], and once again saw increased MYC target gene expression in activated MAIT cells (Figure 2H & Supplementary Figure 3). TCR activation induces MYC expression in conventional $CD8^+$ T cells[26] . Furthermore, MYC expression is maintained by IL-2 through the activation of JAK/STAT signaling pathways[26]. With this in mind we interrogated the upstream signals required for MYC activation in MAIT cells. We compared the ability of TCR stimulation and the cytokines IL-2, IL-12 and IL-18 to induce MYC expression in $MAIT^{IL\text{-}2}$ cells, with TCR triggering induced the strongest MYC expression (Supplementary Figure 4).

[26]. Analysis of the MAIT^{IL-2} proteomic data showed that upon activation, MAIT cells had increased abundance of STAT5 but not STAT3 (Figure 2I-K). Furthermore, inhibition of STAT5 activation reduced MYC expression in TCR-activated MAIT cells (Figure L-M).

MAIT cell proliferation is dependent on MYC

MAIT cells can readily proliferate upon TCR activation with a cognate antigen or bacterial infection[20, 21]. To build on these observations, we investigated the ability of MAIT$^{EX-VIVO}$ cells to proliferate in vitro after stimulation with the riboflavin metabolite 5-ARU, which is further processed into the MAIT cell cognate antigen 5-OP-RU, resulting in a full antigenic stimulation through the TCR. MAIT$^{EX-VIVO}$ cells activated with antigenic stimulation failed to proliferate despite increased expression of activation markers such the interleukin 2 receptor alpha chain, CD25 (Figure 3A-C). Increased expression of CD25 was also noted on MAIT^{IL-2} cells after TCR bead stimulation (Figure 3D). IL-2 is a driver of T cell growth and proliferation[33], so we investigated whether the addition of IL-2 alongside antigenic stimulation could drive MAIT$^{EX-VIVO}$ cell proliferation. Addition of IL-2 resulted in significant MAIT cell growth and proliferation in combination with antigenic stimulation (Figure 3E-G). MYC expression is required for conventional T cell blasting and proliferation in response to TCR signalling[23, 24]. Many of the transcriptional programs driven by MYC are dependent upon dimerization with MAX[34]. The MYC inhibitor 10074-G5 blocks the binding of MAX to MYC and thereby inhibits transcriptional activity[35]. Using this inhibitor, we saw that the increase in cell size and CD25 expression in MAIT cells after TCR simulation was dependent on MYC activity (Figure 3H-I). Furthermore, MYC activity was required for MAIT cell proliferation in response to TCR and IL-2 (Figure 3J & Supplementary Figure 5).

The MYC-controlled amino acid transporter SLC7A5 is required for MAIT cell proliferation.

Proliferation is a metabolically intense process, requiring large amounts of energy and de novo generation of biosynthetic intermediates, so we next investigated metabolic processes under the control of MYC. In conventional murine T cells, TCR-driven

192 expression of MYC induces the expression of critically important amino acid
193 transporters, including SLC7A5[24]. SLC7A5 and its heavy chain chaperone, CD98
194 (SLC3A2), form the heterodimeric large neutral amino acid transporter (LAT-1).
195 Interrogation of the MAIT cell proteomes show that *SLC7A5* expression increases from
196 25000 copies per cell in $MAIT^{IL-2}$ cells to 50000 copies per cell in $MAIT^{IL-2+STIM}$ cells
197 (Figure 4A) which correlates with increased mRNA expression in $MAIT^{IL-2+STIM}$
198 compared with $MAIT^{IL-2}$ cells (Figure 4B). We also noted increased expression of the
199 CD98/SLC3A2 (Figure 4C-D). Together these data show that that upon TCR activation
200 both $MAIT^{EX-VIVO}$ and $MAIT^{IL-2}$ cells increase the expression of SLC7A5 protein, *SLC7A5*
201 mRNA and CD98 surface expression (Figure 4A-C). Using a flow cytometry-based
202 assay, uptake of kynurenine, a fluorescent SLC7A5 substrate, was monitored in MAIT
203 cells. $MAIT^{EX-VIVO}$ cells exhibited low kynurenine uptake, however upon TCR/cytokine
204 stimulation, $MAIT^{EX-VIVO}$ cells rapidly increase transport through SLC7A5 (Figure 4E).
205 From our proteomic analysis we also noted that upon activation MAIT cells increase
206 expression of several other amino acid transporters, including SLC1A5, SLC7A1, and
207 SLC38A1, which are also controlled by MYC[24] (Supplementary Figure 6). We used MYC
208 inhibitors to investigate whether the TCR/cytokine driven increase in LAT-1 expression
209 was dependent upon MYC activity. Inhibition of MYC resulted in reduced *SLC7A5*
210 mRNA expression as well as reduced CD98 expression in activated MAIT cells (Figure
211 4F-G). Furthermore, inhibition of MYC reduced the uptake of the SLC7A5 substrate
212 kynurenine by activated MAIT cells (Figure 4H). Next, we investigated if loss of amino
213 acid transport via LAT-1 impacted MAIT cell proliferation. Using the competitive
214 substrate BCH to block LAT-1 activity, we showed that MAIT cell proliferation is limited
215 when uptake through LAT-1 is blocked. Therefore, SLC7A5 activity during TCR/IL-2
216 activation is required for $MAIT^{EX-VIVO}$ cell proliferation (Figure 4I-K).
217
218 **Glucose metabolism supports MAIT cell proliferation.**
219 MYC has been highlighted as a master regulator of glycolysis[23, 24], and therefore we
220 investigated whether glucose metabolism was required for MAIT cell proliferation. We
221 have reported that MAIT cells had increased glycolytic metabolism upon activation[27],
222 here, we noted increased expression of the glycolytic enzymes (hexokinase-II (HKII)
223 and lactate dehydrogenase (LDH)) in both $MAIT^{EX-VIVO}$ and $MAIT^{IL-2}$ cells following TCR

stimulation (Figure 5A-D). Inhibition of MYC resulted in diminished *HKII* mRNA expression in activated MAIT$^{EX\text{-}VIVO}$ cells (Figure 5E). We also showed that inhibition of MYC limited the rates of glycolytic metabolism in TCR activated MAIT cells (Figure 5F-G). To investigate whether glucose metabolism is required for MAIT cell proliferation, we treated MAIT cells with the glycolytic inhibitor 2-deoxy-D-glucose (2DG). MAIT cell proliferation was inhibited when treated with 2DG (Figure 5H-J). Limiting the glucose availability in the culture media from 10mM to 1mM reduced MAIT cell proliferation (Figure 5K-L). Finally, replacing the carbon source in the culture media from glucose to galactose (which slows the rates of glycolysis[36]) resulted in reduced MAIT cell proliferation (Figure 5M).

MAIT cells from people with obesity display blunted MYC expression and fail to proliferate.

MAIT cell frequencies and cytokine production are altered in people with obesity (PWO)[14, 37, 38]. We investigated the proliferative capacity of MAIT cells from PWO in response to a combination of antigenic (5-ARU-MG) and cytokine (IL-2) stimulation. MAIT cells from PWO displayed defective proliferation in response to immune stimulation when compared to healthy controls (Figure 6A-B, Supplementary Figure 7) . These data provided further evidence that MAIT cells are functionally impacted by obesity. Having highlighted the critical importance of MYC for MAIT cell proliferative responses, we assessed MYC expression in cohorts of PWO and healthy controls, and found impaired induction of MYC expression in MAIT$^{EX\text{-}VIVO}$ cells in response to immune activation from PWO (Figure 6C-D). Targeted analysis of a previously published RNA sequencing data set on MAIT cells isolated from PWO and healthy controls[27], showed reduced expression of MYC target gene expression in MAIT cells from PWO (Figure 6E). *MYC* RNA expression in these same individuals was not reduced (Figure 6F), indicating that signalling downstream of immune activation to drive expression of MYC RNA was not impaired. Since CD25 surface protein expression was reduced with MYC inhibition (Figure 3H), we measured CD25 expression on MAIT cells from PWO, and found diminished CD25 levels in response to TCR and cytokine activation (Figure 6G). Having identified that SLC7A5, a direct transcriptional target of MYC, is critical for MAIT cell proliferation in response to immune stimulation, we

measured SLC7A5 expression on MAIT cells from PWO. We demonstrated that upon activation MAIT cells from PWO express significantly less *SLC7A5* mRNA and CD98, resulting in reduced amino acid transport, a process necessary for proliferation (Figure 6H-J).

Discussion

MAIT cells are a subset of unconventional T cells which are abundant in human blood and tissues, including liver and adipose tissue[6, 39]. MAIT cells are capable of responding rapidly to stimulation by producing cytokines and lytic molecules, and proliferating[6]. Due to their potent effector functions and abundance, MAIT cells have been shown to play an important role in the host defence against pathogens and malignancies[1, 8], and are of interest as a potential immunotherapeutic agent[21, 40]. However, the molecular regulation of MAIT cell effector functions are still emerging. In the current study, we demonstrated that MAIT cell proliferation is dependent on the transcription factor MYC. We showed that upon activation, MAIT cells had a greater abundance of MYC target proteins, including SLC7A5 and HKII, which are both integral to key processes required for MAIT cell proliferation. Finally, we showed that MYC expression and targets under the controls of MYC are defective in people with obesity, underpinning diminished MAIT cell proliferation (Figure 7). These observations suggest a mechanism which may increase host susceptibility to infection and malignancies.

Quantitative mass spectrometry allows a high-dimensional analysis of the proteome and activation induced remodelling[24, 25, 26]. Using this approach, we were able to identify 5740 proteins in both resting IL-2 expanded MAIT cells and stimulated IL-2 expanded MAIT cells, similar to previously published data sets[41, 42]. TCR and cytokine stimulation were associated with the remodelling of the MAIT cell proteome and were associated with significant increases in protein content and cell size. Pathway analysis of our proteomic dataset and previously published RNA sequencing datasets revealed the MYC pathway as one of the most upregulated in MAIT cells. MYC is a critically important transcription factor in conventional T cells, and acts as a metabolic master regulator[23, 24, 26]. Experiments using high-dimensional quantitative mass spectrometry on $CD4^+$ and $CD8^+$ T cells from wild type and MYC deficient mice reveal how MYC

controls TCR-driven cell growth and metabolism[23, 24]. We showed that MYC is a critical regulator of human MAIT cell proliferation.

MAIT cell proliferation was triggered in a two-step process, where activation with 5-ARU-MG, which forms the MAIT cell cognate antigen 5-OP-RU, did not drive MAIT cell proliferation, but did trigger the expression of the high affinity IL-2 receptor, CD25. Subsequent addition of IL-2 drove MAIT cell proliferation. A similar two-step process occurs conventional $CD8^+$ T cells, in which IL-2 not required for the initiation of proliferation but required for sustaining proliferation[43]. We also demonstrated that increased expression of CD25 by activated MAIT cells was dependent on MYC, which aligns with previous reports demonstrating that in MYC deficient conventional T cells, the expression of CD25 does not increase upon stimulation[24].

MYC signalling is also essential for the upregulation of amino acid transporters on T cells, including SLC7A5 [24]. We have previously reported that MAIT cells express SLC7A5[27], and demonstrated here that inhibition of MYC results in diminished SLC7A5 and CD98 expression, and reduced transport of the SLC7A5 substrate kynurenine by activated MAIT cells. Amino acid transport by SLC7A5/CD98 is critical for sustained expression of MYC, suggesting a positive feed-forward loop[24]. Using the SLC7A5 inhibitor BCH we showed that amino acid transport through SLC7A5 is needed for MAIT cell proliferation. This highlights the presence of a MYC-SLC7A5 axis present in activated MAIT cells, similar to that identified in conventional T cells.

MYC also directs a glycolytic metabolism program in conventional T cells[23, 24, 26], that is important for T cell growth, activation and effector functions[44]. Glycolytic metabolism is required for MAIT cell cytokine and lytic molecule production [27, 37, 45], but the factors regulating MAIT cell metabolism and the requirements for MAIT cell proliferation are unknown. Herein we show that MAIT cells increase the expression of key glycolytic enzymes (including HKII and LDH), supporting MAIT cell engagement of glycolytic metabolism upon activation. Furthermore, inhibition of MYC resulted in diminished HKII expression and rates of glycolytic metabolism, confirming that as in conventional T cells, MYC is a key metabolic regulator. In conventional $CD8^+$ T cells,

glucose metabolism is also critical for cell growth and proliferation[46]. Herein we demonstrated that glucose metabolism and glycolysis is needed for optimal MAIT cell proliferation. Limiting glycolysis by acutely reducing glucose availability or substituting glucose with galactose further provided evidence for glucose availability being a rate-limiting step for proliferation in MAIT cells.

MAIT cell cytokine production is defective in numerous human diseases, including cancer, obesity and COVID-19[8, 47, 48]. Here, we showed that MAIT cell proliferation was reduced in people with obesity, which is consistent with reports of defective host protection in obesity. Having demonstrated the importance of MYC and its targets for MAIT cell proliferation, we investigated the impact of obesity on MYC, and observed reduced MYC activity in MAIT cells from people with obesity. Furthermore, we highlight that this is not due to reduced MYC mRNA expression in immune activated MAIT cells from PWO. MYC protein has a short half-life due to constant proteasomal degradation. Increased MYC protein levels are thus only seen in cells with sufficient amino acid transport capable of fuelling protein synthesis in a self-fulfilling feed forward loop[24, 25, 26, 49, 50]. We noted that expression of key MYC targets like SLC7A5 were also defective in MAIT cells isolated from people with obesity, as would be expected with impaired MYC-driven transcription. We have previously demonstrated that defects in glucose metabolism in both MAIT cells and NK cells from people with obesity underlie blunted cytokine production of these cells [27, 28, 29]. The identification of defective MYC expression in MAIT cells from people with obesity helps to further understand these observations.

In conclusion, we have identified MYC as a regulator of MAIT cell metabolism. We demonstrate that a MYC-SLC7A5-glycolysis axis is needed for MAIT cell proliferation and that this is defective in obesity. However, this data extends beyond obesity and provides insight into the molecular and metabolic regulation of MAIT cell proliferation which will have particular relevance for the potential use of MAIT cells for immunotherapy[21].

Materials & methods

Study cohorts & ethical approval A total cohort of 50 adults (25obese/25 non-obese) were recruited. Inclusion criteria included ability to give informed consent, 18-65 years of age and a BMI<28 for the non-obese control cohort and BMI >30 for obese cohort. Exclusion criteria for both cohorts included having a current or recent (<2 weeks) infection, being a current smoker, use of anti-inflammatory medications including GLP-1 analogue therapies. Ethical approval was obtained from both St Vincent's University Medical Ethics Committee and Maynooth University Ethics Committee

Preparation of peripheral blood mononuclear cells (PBMC) and flow cytometric analysis PBMC samples were isolated by density centrifugation over Ficoll from fresh peripheral blood samples. MAIT cell staining was performed using specific surface monoclonal antibodies (All Miltenyi Biotec) namely; CD3 (REA613), CD161 (REA631), CD8 (REA734) and TCRVα7.2 (REA179) (Supplementary Figure 7) in addition to CD25 (REA570), CD71 (REA902) and CD98 (REA387). Cell populations were acquired using a Attune NXT flow cytometer and analysed using FlowJo software (Treestar). Results are expressed as a percentage of the parent population, as indicated and determined using flow minus-1 (FMO) and unstained controls.

MAIT cell proliferation analysis. Fresh PBMC (1 x 10^6 /ml) were stimulated for 18 hours with 1 μg/mL of 5-ARU and 100 μM of Methylglyoxal, in the absence or presence of specific metabolic inhibitors (2DG (2 mM), 10074-G5(10 μM), iBET762(10 μM) or BCH(50 mM)). After 18 hours, RPMI 1640media was replaced with fresh culture media containing IL-2 (33.3 ng/ml). Cultures were maintained for up to 28 days, replacing media with fresh culture media containing IL-2 every 3 days. MAIT cell proliferation was determined by either flow cytometric analysis of MAIT cell frequencies or cell trace violet proliferation assays.

MAIT cell proteomic sample preparation. Purified IL-2 expanded MAIT cells ($MAIT^{IL\text{-}2}$) were stimulated for 18 hours with anti-CD3/CD28 Dynabeads (Thermofisher), IL-12

(50 ng/ml) and IL-18 (50 ng/ml) for 18 hours. Cell pellets were lysed at room temperature in 5% SDS, 50 mM TEAB pH8.5, 10mM TCEP under agitation for 30 mins, then boiled for 5 mins and sonicated with a BioRuptor (30 seconds on, 30 seconds off x 15 cycles). Protein concentration was determined using EZQ protein quantification kit (Invitrogen) according to the manufacturer's protocol. Lysates were alkylated with 20 mM iodoacetamide for 1 hour at room temperature in the dark. The samples were then processed using S-Trap micro columns (Protifi). 12% aqueous phosphoric acid was added at 1:10 to each sample for a final concentration of ~1.2% phosphoric acid. Samples were transferred to 5 ml lo-bind microcentrifuge tubes (Eppendorf). 3200µl of S-Trap binding buffer (100 mM TEAB - pH 7.1 adjusted using phosphoric acid, 90% MeOH) was added to each sample. Each sample was loaded onto an S-Trap column in batches of 165 µl and centrifuged at 4,000 xg for 30 s or until all SDS lysate/S-Trap buffer had passed through the S-Trap column. Loading and centrifuging of columns was repeated until all the lysate was run through the column. Captured protein was then washed by adding 150 µl S-trap binding buffer to columns, which were then spun at 4,000 g for 30 s: columns were washed five times in total. Columns were transferred to fresh 2ml collection tubes. 20 µl of digestion buffer (50mM ammonium bicarbonate in HPLC water) containing 1:20 trypsin was added onto each column. Samples were centrifuged at 4000g for 30 seconds and any solution that passed through was returned to the top of the column. Tubes were incubated for 2 hrs at 47°C. 40 µL of digestion buffer containing trypsin was added to each column. Samples were centrifuged at 1,000 xg for 60 sec and the peptide elution kept. 40 µL of 0.2% aqueous formic acid was added to the S-Trap protein-trapping matrix and centrifuged at 1,000 x g for 60 sec into the same collection tube. 40 µL of 50% aqueous acetonitrile containing 0.2% formic acid was added and samples centrifuged at 4000 x g for 60 seconds for a final elution.

Data independent acquisition (DIA) mass spectrometry acquisition. An equivalent of 1.5 µg peptides were injected onto a nanoscale C18 reverse-phase chromatography column coupled to an UltiMate 3000 RSLC nano, HPLC system (Thermo Fisher) and an Orbitrap Exploris 480 Mass Spectrometer (Thermo Fisher). For liquid chromatography the following buffers were used: buffer A (0.1% formic acid in Milli-Q water (v/v)) and

buffer B (80% acetonitrile and 0.1% formic acid in Milli-Q water (v/v). Samples were loaded at 10 µL/min onto a trap column (100 µm × 2 cm, PepMap nanoViper C18 column, 5 µm, 100 Å, Thermo Scientific) equilibrated in 0.1% trifluoroacetic acid (TFA). The trap column was washed for 3 min at the same flow rate with 0.1% TFA then switched in-line with a Thermo Scientific, resolving C18 column (75 µm × 50 cm, PepMap RSLC C18 column, 2 µm, 100 Å). Peptides were eluted from the column at a constant flow rate of 300 nl/min with a linear gradient from 3% buffer B to 6% buffer B in 5 min, then from 6% buffer B to 35% buffer B in 115 min, and finally to 80% buffer B within 7 min. The column was then washed with 80% buffer B for 4 min and re-equilibrated in 3% buffer B for 15 min. Two blanks were run between each sample to reduce carry-over. The column was kept at a constant temperature of 50°C.

The data was acquired using an easy spray source operated in positive mode with spray voltage at 2.6 kV, and the ion transfer tube temperature at 250°C. The MS was operated in DIA mode. A scan cycle comprised a full MS scan (m/z range from 350-1650), with RF lens at 40%, AGC target set to custom, normalised AGC target at 300%, maximum injection time mode set to custom, maximum injection time at 20 ms, microscan set to 1 and source fragmentation disabled. MS survey scan was followed by MS/MS DIA scan events using the following parameters: multiplex ions set to false, collision energy mode set to stepped, collision energy type set to normalized, HCD collision energies set to 25.5, 27 and 30%, orbitrap resolution 30000, first mass 200, RF lens 40%, AGC target set to custom, normalized AGC target 3000%, microscan set to 1 and maximum injection time 55 ms. Data for both MS scan and MS/MS DIA scan events were acquired in profile mode. The method used for the DIA mass spectrometry was based on a previously published approach[51].

DIA data quantification and analysis. Quantification of reporter ions was completed using Spectronaut (VX, Biognosys; Spectronaut 15.2.210819.50606) in library-free (directDIA) mode. Minimum peptide length was set to 7 and maximum peptide length was set to 52, with a maximum of 2 missed cleavages. MS1 and MS2 mass tolerance strategy and XIC IM and RT extraction windows were set to dynamic, all with a correction factor of 1. Trypsin was specified as the digestive enzyme used. The false

discovery rate at the precursor ion level and protein level was set at 1% (protein and precursor Q-value cut-off). The max number of variable modifications was set to 5, with protein N-terminal acetylation, and glutamine and asparagine deamidation set as variable modifications. Carbamidomethylation of cysteine residues was selected as a fixed modification. For calibration, the MS1 and MS2 mass tolerance strategy was set to the system default. Machine learning was set to across experiment, with a precursor PEP cut-off of 0.2, a protein Q-value cut-off of 0.01. Single-hit proteins were not excluded, with single-hits defined by stripped sequence. For quantification, the quantification method was set to QUANT 2.0. Inference correction was set to true with MS1 min of 2 and MS2 min of 3. The major protein grouping was by protein group ID and the minor peptide grouping was set to stripped sequence. Major and minor group top N was set to false, with minor and major group quantities set to sum precursor quantity and sum peptide quantity respectively. Quantity at the MS-level was set to MS2 and quantity type to area. Proteotypicity filter was set to none, data filtering to Q-value and cross run normalisation was switched off. MS2 demultiplexing was automatic, the run limit for the directDIA library set to -1, with no profiling strategy or unify peptide peaks strategy. Data filtering and protein copy number quantification was performed in the Perseus software package, version 1.6.6.0. Copy numbers were calculated using the proteomic ruler[30]. This method sets the summed peptide intensities of the histones to the number of histones in a typical diploid cell. The ratio between the histone peptide intensity and summed peptide intensities of all other identified proteins is then used to estimate the protein copy number per cell for all the identified proteins. Further filtration of the data was completed to include proteins detected in at least ≥ 2 biological replicates, and exclude proteins identified based on single peptides.

Cell trace violet proliferation assay. MAIT cell proliferation was also measured using a CellTrace™ Violet (CTV) proliferation kit (ThermoFisher) according to the manufacturer's instructions. Briefly, CellTrace solution was prepared immediately prior to use to 5 mM stock using DMSO. Next the dye for diluted to 5 µM working concentration by adding appropriate amount of the stock solution into pre-warmed PBS. Isolated PBMC were stained at 10^6 cells per mL of the PBS-dye solution. Cells

were incubated for 20 min at room temperature, protected from light with circular agitation. Unbound dye was washed away with RPMI1640, and cell were incubated for at least 10 minutes to allow acetate hydrolysis of the dye. CTV stained cells were stimulated for 18 hours with 1 μg/mL of 5-ARU and 100μM of methylglyoxal, in the absence or presence of specific metabolic inhibitors (2DG (2mM), 10074-G5(10uM), iBET762 (25 nM) or BCH (50 mM)). After 18 hours, media was replaced with fresh culture media containing IL-2 (33.3 ng/ml). Cultures were maintained for 5 days before analysis.

MAIT cell metabolic analysis. Fresh PBMC (1 x 10^6 /ml) or $MAIT^{IL\text{-}2}$ cells were activated using Dynabeads, IL-12 (50 ng/ml) and IL-18 (50 ng/ml) for 18 hours. Cells were then labelled for extracellular markers, then fixed and permeabilized using the True-Nuclear Transcription Factor Buffer set (BioLegend) according to the manufacture's instructions before intracellular staining with monoclonal antibodies specific for hexokinase II (Abcam EPR20839), lactate dehydrogenase (Abcam EP1563Y) or MYC (Cell Signalling D84C12).

MAIT cell Seahorse experiments. For real-time analysis of the extracellular acidification rate (ECAR) of $MAIT^{IL\text{-}2}$ cells were cultured in the absence or presence of stimulation (Dynabead, IL-12 & IL-18 (both 50 ng/ml) and the MYC inhibitor iBET762 (25 mM) for 18 hours before analysis on a Seahorse XF-96 Analyzer (Seahorse Bioscience). In brief, 200,000 MAIT cells were adhered to a CellTaq (BD Pharmingen) coated 96-well XF Cell Culture Microplate (Seahorse Biosciences). Sequential measurements of ECAR following addition of the inhibitors (Sigma) oligomycin (2 μM) and 2-deoxyglucose (2DG, 30 mM) allowed for the calculation of basal glycolysis. Each cell culture condition was evaluated in quadruplicate, and 14 measurements were made per sample.

MAIT cell Kynurenine and BCH experiments. MAIT cells activated for 18 hours (Dynabeads and IL-12/IL-18 – both 50 ng/ml) in the absence or presence of a MYC inhibitor (iBET 762 25 nM) were washed and resuspended in 200ml warmed HBSS (1x10^6 cells) and incubated in a water bath at 37°C. Kynurenine (200 mM, in HBSS) was

warmed to 37°C, with a 4°C control and added as appropriate. Uptake was stopped after 4 minutes by PFA (Final concentration 1%) for 30 mins at room temperature, in the dark. After fixation, wash cells twice in PBS/0.5% BSA and resuspend in PBS/0.5% BSA prior to acquisition on flow cytometer. The 405nm laser and 450/50 BP filter were used for kynurenine fluorescence detection. For SLC7A5 inhibition experiments, the concentration of amino acids in RPMI was diluted twofold using Hank's balanced salt solution (HBSS; Invitrogen) in the presence or absence of BCH (50 mM; Sigma).

PCR gene expression. mRNA was extracted from MAIT cells from healthy controls and PWO using EZNA Total RNA kit I (Omegabio-tek) according to the manufacturer's protocol. Synthesis of cDNA was performed using qScript cDNA Synthesis kit (QuantaBio). Real time RT-qPCR was performed using PerfeCTa SYBR Green FastMix Reaction Mix (Green Fastmix, ROX^{TM}) (QuantaBio) and KiCqStart primer sets (Sigma).

Western blotting analysis. Human MAIT^{IL-2} cells ($2.5x10^6$) were cultured in 24-well plates stimulated with various stimuli (Dynabeads, IL-2 (10-40 ng/ml) IL-12 (50 ng/ml) and IL-18 (50 ng/ml) for 18 hours (in the absence or presence of STAT5 inhibitor (CAS 285986-31-4 Merck)) before harvesting for western blotting. Cells were lysed in NP-40 lysis buffer (50mM Tris-HCl, pH 7.4, containing 150 mM NaCl, 1% (w/v) IGEPAL (Sigma), and complete protease inhibitor mixture (Roche)). Samples were resolved using SDS-PAGE and transferred to nitrocellulose membranes before analysis with anti-MYC (Cell Signalling) anti-β-Actin (Sigma) antibodies. Protein bands were visualised using enhanced chemiluminescence.

In silico RNA sequencing analysis. Publicly available RNA sequencing data sets of MAIT cells were downloaded from Gene Expression Omnibus (GEO) accession number GSE123805[11] (Hinks *et al.,* 2019) and National Center for Biotechnology Information (NCBI) Sequence Read Archive (SRA) accession number PRJNA559574 [10]. Raw read counts were downloaded from GEO[11] and the data analysis pipeline to this point is detailed in the associated paper. Whereas raw sequencing data in format of FASTQ files were downloaded from the NCBI SRA [10] and the following data analysis pipeline was implemented. The TrimGalore (v0.6.6) tool was used with Cutadapt (v1.15) and

FastQC to apply quality and adapter trimming to FASTQ files. STAR (v2.7.9a) was used to align trimmed reads to the human genome (*Homo sapiens* high coverage assembly GRCh38 from the Genome Reference Consortium – GRCh38.p13) with the quantMode GeneCounts option to output read counts per gene. The Bioconductor package EdgeR (v3.28.1) was applied in R (v3.6.3) to identify statistically significant differentially expressed genes between patient groups. Biological and technical variation was accounted for by the negative binomial distribution of RNAseq count data using a generalization of the Poisson distribution model. The filterByExpr function was applied to remove lowly expressed genes. The data was normalized across library sizes, between samples using the trimmed mean of M-values (TMM) normalization method. Tagwise dispersions were estimated for the normalized dataset. *P*-values from multiple comparisons were corrected with the Benjamini-Hochberg method in EdgeR. For the comparisons between stimulations and controls, genes were considered significantly differentially expressed with an FDR adjusted *p*-value < 0.1. Variance Modeling at the Observational Level (VOOM) method within edgeR was used to output normalized read counts as LogCPM values. These were used to perform hierarchical clustering and to construct heatmaps in Gene Pattern's online server (v3.9.11) and to perform Gene Set Enrichment Analysis (GSEA) (v4.1.0) with annotated HALLMARK genesets from the MSigDB (Molecular Signatures Database) collections (v6.2). Venn diagrams were constructed using InteractiVenn[52].

Statistics. Statistical analysis was completed using Graph Pad Prism 6 Software (USA). Data is expressed as SEM. We determined differences between two groups using student t-test and Mann Whitney U test where appropriate. Analysis across 3 or more groups was performed using ANOVA. Correlations were determined using linear regression models and expressed using Pearson or Spearman's rank correlation coefficient, as appropriate. P values were expressed with significance set at <0.05.

REFERENCES

1. Godfrey, D.I., Koay, H.F., McCluskey, J. & Gherardin, N.A. The biology and functional importance of MAIT cells. *Nat Immunol* **20**, 1110-1128 (2019).

2. Le Bourhis, L. *et al.* Antimicrobial activity of mucosal-associated invariant T cells. *Nat Immunol* **11**, 701-708 (2010).

3. van Wilgenburg, B. *et al.* MAIT cells are activated during human viral infections. *Nature communications* **7**, 11653 (2016).

4. Treiner, E. *et al.* Selection of evolutionarily conserved mucosal-associated invariant T cells by MR1. *Nature* **422**, 164-169 (2003).

5. Kjer-Nielsen, L. *et al.* MR1 presents microbial vitamin B metabolites to MAIT cells. *Nature* **491**, 717-723 (2012).

6. Provine, N.M. & Klenerman, P. MAIT Cells in Health and Disease. *Annu Rev Immunol* **38**, 203-228 (2020).

7. Gapin, L. Check MAIT. *J Immunol* **192**, 4475-4480 (2014).

8. O'Neill, C., Cassidy, F.C., O'Shea, D. & Hogan, A.E. Mucosal Associated Invariant T Cells in Cancer-Friend or Foe? *Cancers (Basel)* **13** (2021).

9. Leng, T. *et al.* TCR and Inflammatory Signals Tune Human MAIT Cells to Exert Specific Tissue Repair and Effector Functions. *Cell reports* **28**, 3077-3091.e3075 (2019).

10. Lamichhane, R. *et al.* TCR- or Cytokine-Activated CD8. *Cell reports* **28**, 3061-3076.e3065 (2019).

11. Hinks, T.S.C. *et al.* Activation and In Vivo Evolution of the MAIT Cell Transcriptome in Mice and Humans Reveals Tissue Repair Functionality. *Cell reports* **28**, 3249-3262 e3245 (2019).

12. Slichter, C.K. *et al.* Distinct activation thresholds of human conventional and innate-like memory T cells. *JCI insight* **1** (2016).

13. Chiba, A. *et al.* Mucosal-associated invariant T cells promote inflammation and exacerbate disease in murine models of arthritis. *Arthritis Rheum* **64**, 153-161 (2012).

14. Carolan, E. *et al.* Altered distribution and increased IL-17 production by mucosal-associated invariant T cells in adult and childhood obesity. *J Immunol* **194**, 5775-5780 (2015).

15. Cosgrove, C. *et al.* Early and nonreversible decrease of CD161++ /MAIT cells in HIV infection. *Blood* **121**, 951-961 (2013).

16. Leeansyah, E. *et al.* Activation, exhaustion, and persistent decline of the antimicrobial MR1-restricted MAIT-cell population in chronic HIV-1 infection. *Blood* **121**, 1124-1135 (2013).

17. Kang, S.J. *et al.* Activation, Impaired Tumor Necrosis Factor-alpha Production, and Deficiency of Circulating Mucosal-Associated Invariant T Cells in Patients with Scrub Typhus. *PLoS Negl Trop Dis* **10**, e0004832 (2016).

18. Bergin, R. *et al.* Mucosal-associated invariant T cells are associated with insulin resistance in childhood obesity, and disrupt insulin signalling via IL-17. *Diabetologia* (2022).

19. Gutierrez-Arcelus, M. *et al.* Lymphocyte innateness defined by transcriptional states reflects a balance between proliferation and effector functions. *Nature communications* **10**, 687 (2019).

20. Howson, L.J. *et al.* MAIT cell clonal expansion and TCR repertoire shaping in human volunteers challenged with Salmonella Paratyphi A. *Nature communications* **9**, 253 (2018).

21. Parrot, T. *et al.* Expansion of donor-unrestricted MAIT cells with enhanced cytolytic function suitable for TCR-redirection. *JCI insight* (2021).

22. Newsholme, E.A., Crabtree, B. & Ardawi, M.S. The role of high rates of glycolysis and glutamine utilization in rapidly dividing cells. *Biosci Rep* **5**, 393-400 (1985).

23. Wang, R. *et al.* The transcription factor Myc controls metabolic reprogramming upon T lymphocyte activation. *Immunity* **35**, 871-882 (2011).

24. Marchingo, J.M., Sinclair, L.V., Howden, A.J. & Cantrell, D.A. Quantitative analysis of how Myc controls T cell proteomes and metabolic pathways during T cell activation. *Elife* **9** (2020).

25. Sinclair, L.V. *et al.* Control of amino-acid transport by antigen receptors coordinates the metabolic reprogramming essential for T cell differentiation. *Nat Immunol* **14**, 500-508 (2013).

26. Preston, G.C. *et al.* Single cell tuning of Myc expression by antigen receptor signal strength and interleukin-2 in T lymphocytes. *The EMBO journal* **34**, 2008-2024 (2015).

27. O'Brien, A. *et al.* Obesity Reduces mTORC1 Activity in Mucosal-Associated Invariant T Cells, Driving Defective Metabolic and Functional Responses. *J Immunol* **202**, 3404-3411 (2019).

28. Tobin, L.M. *et al.* NK cells in childhood obesity are activated, metabolically stressed, and functionally deficient. *JCI insight* **2** (2017).

29. Michelet, X. *et al.* Metabolic reprogramming of natural killer cells in obesity limits antitumor responses. *Nat Immunol* **19**, 1330-1340 (2018).

30. Wisniewski, J.R., Hein, M.Y., Cox, J. & Mann, M. A "proteomic ruler" for protein copy number and concentration estimation without spike-in standards. *Mol Cell Proteomics* **13**, 3497-3506 (2014).

31. Howden, A.J.M. *et al.* Quantitative analysis of T cell proteomes and environmental sensors during T cell differentiation. *Nat Immunol* **20**, 1542-1554 (2019).

32. Hukelmann, J.L. *et al.* The cytotoxic T cell proteome and its shaping by the kinase mTOR. *Nat Immunol* **17**, 104-112 (2016).

33. Cornish, G.H., Sinclair, L.V. & Cantrell, D.A. Differential regulation of T-cell growth by IL-2 and IL-15. *Blood* **108**, 600-608 (2006).

34. Amati, B. *et al.* Oncogenic activity of the c-Myc protein requires dimerization with Max. *Cell* **72**, 233-245 (1993).

35. Yap, J.L. *et al.* Pharmacophore identification of c-Myc inhibitor 10074-G5. *Bioorg Med Chem Lett* **23**, 370-374 (2013).

36. Grimm, D. *et al.* Modulation of cellular energetics by galactose and pioglitazone. *Cell Tissue Res* **369**, 641-646 (2017).

37. Brien, A.O. *et al.* Targeting mitochondrial dysfunction in MAIT cells limits IL-17 production in obesity. *Cell Mol Immunol* (2020).

38. Magalhaes, I. *et al.* Mucosal-associated invariant T cell alterations in obese and type 2 diabetic patients. *J Clin Invest* **125**, 1752-1762 (2015).

39. Toubal, A., Nel, I., Lotersztajn, S. & Lehuen, A. Mucosal-associated invariant T cells and disease. *Nat Rev Immunol* (2019).

40. Godfrey, D.I., Le Nours, J., Andrews, D.M., Uldrich, A.P. & Rossjohn, J. Unconventional T Cell Targets for Cancer Immunotherapy. *Immunity* **48**, 453-473 (2018).

41. Schubert, K. *et al.* A Multi-Omics Analysis of Mucosal-Associated-Invariant T Cells Reveals Key Drivers of Distinct Modes of Activation. *Front Immunol* **12**, 616967 (2021).

42. Bulitta, B. *et al.* Proteomic definition of human mucosal-associated invariant T cells determines their unique molecular effector phenotype. *Eur J Immunol* **48**, 1336-1349 (2018).

43. D'Souza, W.N. & Lefrançois, L. IL-2 is not required for the initiation of CD8 T cell cycling but sustains expansion. *J Immunol* **171**, 5727-5735 (2003).

44. O'Neill, L.A., Kishton, R.J. & Rathmell, J. A guide to immunometabolism for immunologists. *Nat Rev Immunol* **16**, 553-565 (2016).

45. Zinser, M.E. *et al.* Human MAIT cells show metabolic quiescence with rapid glucose-dependent upregulation of granzyme B upon stimulation. *Immunol Cell Biol* (2018).

46. Sanchez, J., Jackson, I., Flaherty, K.R., Muliaditan, T. & Schurich, A. Divergent Impact of Glucose Availability on Human Virus-Specific and Generically Activated CD8 T Cells. *Metabolites* **10** (2020).

47. Magalhaes, I., Kiaf, B. & Lehuen, A. iNKT and MAIT Cell Alterations in Diabetes. *Front Immunol* **6**, 341 (2015).

48. McCarthy, C., O'Donnell, C.P., Kelly, N.E.W., O'Shea, D. & Hogan, A.E. COVID-19 severity and obesity: are MAIT cells a factor? *Lancet Respir Med* **9**, 445-447 (2021).

49. Swamy, M. *et al.* Glucose and glutamine fuel protein O-GlcNAcylation to control T cell self-renewal and malignancy. *Nat Immunol* **17**, 712-720 (2016).

50. Sinclair, L.V. *et al.* Antigen receptor control of methionine metabolism in T cells. *Elife* **8** (2019).

51. Muntel, J. *et al.* Surpassing 10 000 identified and quantified proteins in a single run by optimizing current LC-MS instrumentation and data analysis strategy. *Mol Omics* **15**, 348-360 (2019).

52. Heberle, H., Meirelles, G.V., da Silva, F.R., Telles, G.P. & Minghim, R. InteractiVenn: a web-based tool for the analysis of sets through Venn diagrams. *BMC Bioinformatics* **16**, 169 (2015).

Acknowledgements: The authors would like to thank all the donors and patients for supporting this project.

Funding Source: This study is supported by the National Children's Research Centre. NKM is supported by Health Research Board (ILP-POR-2019-110). CB is supported by a fellowship from Irish Research Council. Financial support for the Attune NxT was provided to Maynooth University Department of biology by Science Foundation Ireland (16/RI/3399). The proteomic research was supported by a Wellcome Trust Equipment Award to Prof Doreen A. Cantrell (202950/Z/16/Z).

Contributors Statement: NKM, MMP, CR, RB, NAW, CDB and CON performed the experiments and carried out analysis and approved the final manuscript as submitted. NV and GSB provided MAIT cell reagents and aided in the design of MAIT cell activation experiments. CF performed the in silico RNA sequencing analysis. NWK and DOS recruited patient cohorts and provided relevant clinical data. AEH, NJ, DOS & LVS

conceptualized and designed the study, analyzed the data, drafted the manuscript, and approved the final manuscript as submitted.

Competing Interest: The authors declare no conflict of interest.

Data Availability: All data needed to evaluate the conclusions in the paper are present in the paper or the Supplementary Materials. All data is available from the corresponding author in line with ethical approval. Proteomic Data is deposited at XXXX

Figure Legends

Figure 1. Remodelling of MAIT cell proteome after activation. (A) Proteins from IL-2 expanded MAIT ($MAIT^{IL-2}$) cells were ranked by mass contribution and the mean cumulative protein mass was plotted against protein rank (n=4). (B) Table outlining the total number of proteins detected in $MAIT^{IL-2}$ cells and their change upon stimulation ($MAIT^{STIM}$; 18 hours with antiCD3/CD28 beads and 50ng/ml IL-12 & IL-18) using quantitative proteomics (n=4 per group). (C) Protein mass in $MAIT^{IL-2}$ or $MAIT^{STIM}$(n=4). (D) Scatter plot showing ex vivo MAIT cell size (Forward scatter) basally or stimulated (as above)(n=15). (E) Heatmap of the proteome of $MAIT^{IL-2}$ and $MAIT^{STIM}$ cells (as above) (n=4/group). Relative protein abundance is graded from blue (low) to red (high) per row. Key MAIT cell proteins (IL-18R1, KLRB1, DPPIV & TRAV1-2) are represented in scatter graphs and their position in the heatmap is denoted by arrows)(n=4/group). (F) Scatter plot displaying the copy numbers against fold change of the $MAIT^{STIM}$ cell proteome compared with $MAIT^{IL-2}$ (Green circles represent proteins increased more than 1.5 fold over $MAIT^{IL-2}$ cells). (G) Pie chart showing proportional pathway analysis based on the $MAIT^{STIM}$ cell proteome (Analysis performed with Panther – Raw data in supplementary file 1). * $p<0.05$, ** $p<0.01$ and *** $p<0.001$.

Figure 2. Activation of MYC and its target pathways in MAIT cells. (A) GSEA plot showing the increase in MYC targets gene expression in activated MAIT cells. Data extrapolated from previously published RNA sequence dataset[10] on ex vivo MAIT cells stimulated through TCR. (B) Heatmap displaying expression amounts of MYC-target in basal ($MAIT^{IL-2}$) or stimulated ($MAIT^{STIM}$; 18hr antiCD3/CD28 beads + 50ng/ml IL-12 & IL-18) cells as determined by quantitative proteomics (n=4 per group). Relative protein abundance is graded from grey (low) to green (high) per row. (C) Proteomic determination of MYC protein expressed as copies per cell from basal ($MAIT^{IL-2}$) or stimulated ($MAIT^{STIM}$) cells (n=4 per group) (Note identification based on single peptide hit). (D-E) Western blot and densitometry displaying MYC expression in $MAIT^{IL-2}$ or stimulated (as above) $MAIT^{STIM}$ cells (n=4). (F-G) Representative flow cytometry histogram (F) (Mean Fluorescence Intensity (MFI) values are shown within histogram) and MFI values (G) of MYC expression in $MAIT^{EX\ VIVO}$ cells (black) or $MAIT^{STIM}$ (green) (n=4). (H) Heatmap displaying MYC target genes in $MAIT^{EX\ VIVO}$ cells with or without TCR stimulation. Data extrapolated from previously published RNA

sequence dataset[11]. (I-K) Scatter plots showing STAT3, STAT5a, STAT5b protein levels expressed as copies per cell from basal ($MAIT^{IL-2}$) or stimulated ($MAIT^{STIM}$) cells (n=4/group). (L-M) Western blot and densitometry displaying MYC expression in $MAIT^{IL-2}$ or $MAIT^{STIM}$ cells in the absence or presence of a STAT5i (n=3). * p<0.05, ** p<0.01 and *** p<0.001.

Figure 3. IL-2 driven proliferation of MAIT cells is dependent on MYC. (A) The frequency of MAIT cells (as a percentage of total T cells) after stimulation of PBMC ($1x10^6$) with antigenic stimulation (cognate antigen 5-ARUand Methylglyoxal) for 7 days (n=6). (B-C) Representative flow cytometry histogram and scatter plot showing CD25 (IL-2RA) expression on $MAIT^{ex\ vivo}$ or stimulated through the TCR using antiCD3/CD28 beads/IL-12 & IL18 ($MAIT^{STIM}$) for 18 hours (n=9). (D) CD25 protein expressed as copies per cell from $MAIT^{IL-2}$ cells basally or $MAIT^{STIM}$ (n=4). (E) Graph demonstrating frequency of MAIT cells (represented as percentage of T cells) after stimulation with 5-ARU (1ug/ml) and Methylglyoxal (100μM) in the absence or presence of IL-2 (33.3ng/ml) for 7 days (n=5). (F-G) Representative flow cytometry dot plot and scatter plot showing MAIT cell frequencies after 7 days stimulation with 5-ARU, Methylglyoxal and IL-2 (n=10). (H) MFI of CD25 expression on MAIT cells after 18 hours stimulation (as in C) in the absence or presence of the MYC inhibitor (10074-G5, 10uM) (n=5). (I) $MAIT^{IL-2}$ cell frequency after 7 days expansion (as in E) in the absence of presence of the MYC inhibitor 10074-G5 (10uM) (n=8). (J) Forward scatter MFI of MAIT cells after stimulation (as in C) in the absence of presence of the MYC inhibitor 10074-G5 (n=5). * p<0.05, ** p<0.01 and *** p<0.001.

Figure 4. SLC7A5 facilitates MAIT cell proliferation and is dependent on MYC. (A) Mean protein copy number per cell of SLC7A5 in $MAIT^{IL-2}$ cells and in cells stimulated for 18hrs ($MAIT^{STIM}$; antiCD3/CD28 beads/IL-12 & IL18) (n=4). (B) Scatter plot showing SLC7A5 mRNA expression in $MAIT^{IL-2}$ cells or $MAIT^{STIM}$ (as in A) (n=12). (C) Flow cytometry MFI data of CD98 expression on ex vivo MAIT cells or stimulated for 18 hrs (as in A)(n=7). (D) Mean protein copy number per cell of SLC3A52 in basal or stimulated $MAIT^{IL-2}$ cells (n=4/group). (E) Flow cytometry data of uptake of kynurenine into ex vivo MAIT cells (n=5). (F) SLC7A5 mRNA expression in $MAIT^{IL-2}$ cells and $MAIT^{STIM}$ (as in A) in the absence or presence of the MYC specific inhibitor 10074-G5 (n=5). (G) Flow cytometry MFI expression of CD98 on ex vivo MAIT cells after stimulation (as in A) in the absence or presence of the MYC specific inhibitor 10074-G5 (10uM) (n=5). (H) Flow cytometry data of uptake of kynurenine into $MAIT^{IL-2}$ cells stimulated for 18 hours (antiCD3/CD28 beads/IL-12 & IL18) in the absence or presence of the MYC inhibitor iBET 762 (n=4). (I) The frequency of MAIT cells after 7 days expansion with 5-ARU (1ug/ml) and Methylglyoxal (100μM) in the absence or presence of IL-2 (33.ng/ml)) in the absence of presence of the SLC7A5 inhibitor BCH (n=5). (J-K) Representative flow cytometry histogram and scatter plot showing cell trace violet (CTV) MFI in MAIT cells after 5 days stimulation (as in G) in the absence of presence of BCH (n=7). * p<0.05, ** p<0.01 and *** p<0.001.

Figure 5. Glucose metabolism facilitates MAIT cell proliferation and is dependent on MYC. (A) Mean protein copy number per cell of Hexokinase-II (HKII) in $MAIT^{IL-2}$ and in

$MAIT^{IL2+STIM}$ (stimulated for 18 hours with antiCD3/CD28 beads and IL-18 (50ng/ml) (n=4). (B-C) Representative flow cytometry histogram and MFI data of HKII in $MAIT^{ex\text{-}vivo}$ cells basally or stimulated (18 hours with antiCD3/CD28 beads and IL-18 (50ng/ml); $MAIT^{STIM}$)(n=8). (D) Flow cytometry MFI data of LDHA expression in $MAIT^{ex\text{-}vivo}$ and $MAIT^{STIM}$ cells (as in C) (n=8). (E) HKII mRNA expression in $MAIT^{IL\text{-}2}$ and in $MAIT^{IL2+STIM}$ cells (as in A) in the absence of presence of the MYC specific inhibitor 10074-G5 (n=5). (F-G) Representative Seahorse Analyzer trace and scatter plot detailing the ECAR rates of $MAIT^{IL\text{-}2}$ cells stimulated for 18 hours (antiCD3/CD28 beads/IL-12 & IL18) in the absence or presence of the MYC inhibitor iBET 762 (n=4). (H) The frequency of MAIT cells after 7 days expansion from PBMC ($1x10^6$) using cognate antigen 5-ARU (1ug/ml), Methylglyoxal (100μM) and IL-2 (33.3ng/ml) in the absence of presence of the glycolysis inhibitor 2DG (2mM) (n=5). (I-J) Representative flow cytometry histogram and scatter plot showing cell trace violet (CTV) MFI in MAIT cells after 5 days stimulation in the absence of presence of 2DG (n=5). (K-L) Representative flow cytometry dot plot and MAIT cell frequencies after 7 days stimulation in media containing either 10mM or 1mM glucose (n=3). (M) MAIT cell frequencies after 7 days stimulation in media containing either 10mM glucose or 10mM galactose (n=6). * p<0.05, ** p<0.01 and *** p<0.001.

Figure 6. MYC is defective in obesity resulting in diminished MAIT cell proliferation. (A) The frequency of MAIT cells after 0-28 days expansion after 18 hour stimulation with 5-ARU (1ug/ml), Methylglyoxal (100μM) and maintenance in IL-2 (33.3ng/ml) in either healthy controls (green circles) or people with obesity (PWO) (grey circles) (n=10/group). (B) Fold expansion of MAIT cells from healthy controls or people with obesity after 7 days stimulation (with 5-ARU (1ug/ml), Methylglyoxal (100μM) and IL-2 (33.3ng/ml)) (n=8). (C-D) Representative flow cytometry histogram (C) and MFI data (D) of MYC expression in ex vivo MAIT cells from healthy controls (top panel,C) or PWO (bottom panel,C) stimulated with antiCD3/CD28 beads and IL-18 (50ng/ml) for 18 hours (n=6-7/group). (E) Scatter graph showing MYC gene counts (extrapolated from published RNA sequencing dataset[27]) in ex-vivo MAIT cells from health controls or PWO (n=4-5/group). (F) Heatmap displaying MYC target genes in ex-vivo MAIT cells from health controls or PWO (n=4-5/group). (G) CD25 expression (MFI) on ex-vivo MAIT cells or stimulated MAIT cells (as in C) from either healthy controls or PWO (n=5-8/group). (H) mRNA expression of *Slc7a5* in $MAIT^{IL\text{-}2}$ cells or $MAIT^{IL\text{-}2}$ stimulated (as in C) from either healthy controls or PWO (n=6-10/group). (I) Scatter plot showing CD98 expression (MFI) on ex-vivo MAIT cells basally or stimulated (as in C) from either healthy controls or PWO (n=3-4/group). (J) Scatter plot showing Kynurenine uptake into MAIT cells from either healthy controls or PWO (n=5/group). * p<0.05, ** p<0.01 and *** p<0.001.

Figure 7. Working Model. Schematic outlining the proposed working model. Top panel details a MYC-SLC7A5-Glycolysis axis in activated MAIT cells. Bottom panel outlines the impact of obesity on the proposed MYC-SLC7A5-Glycolysis axis in activated MAIT cells.

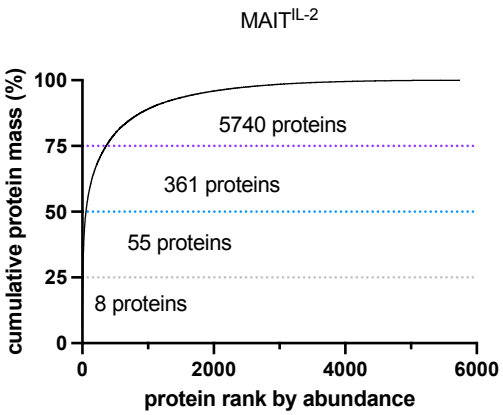

B.

MAIT IL2 -> MAIT STIM	
Total Proteins Detected (Avg)	5740
Increasing (>1.5 fold change, p = 0.05)	~780
Decreasing (>0.5 fold change, p = 0.05)	~65

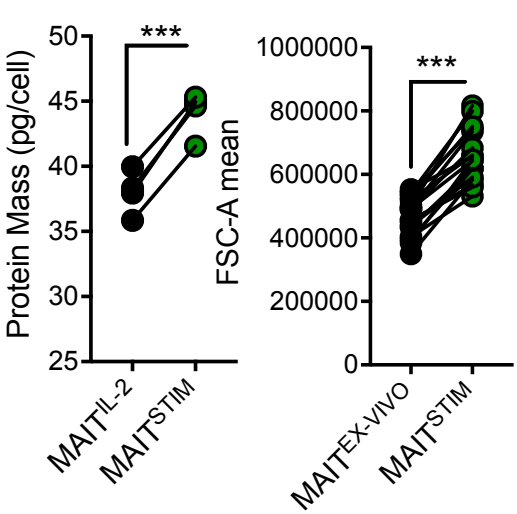

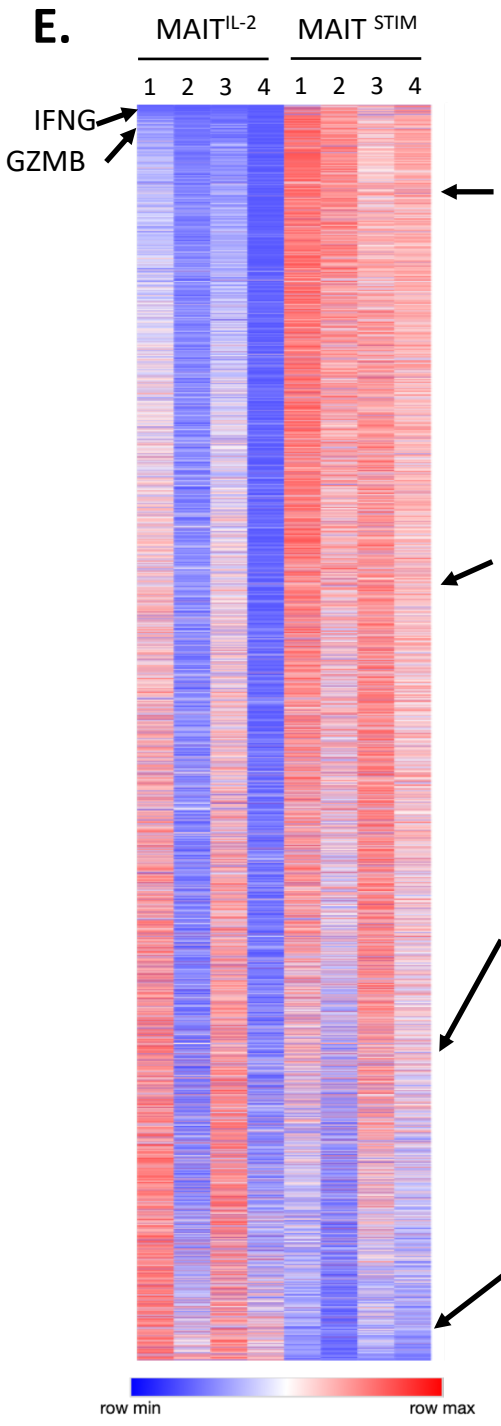

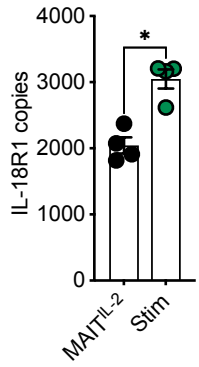

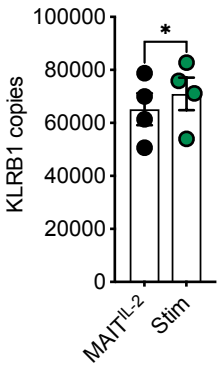

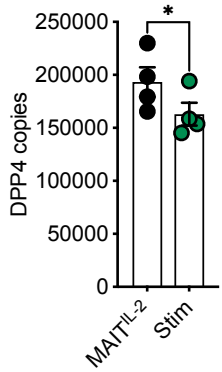

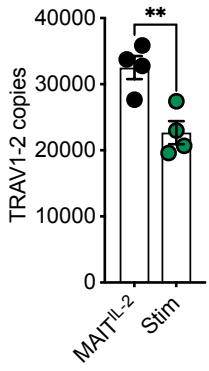

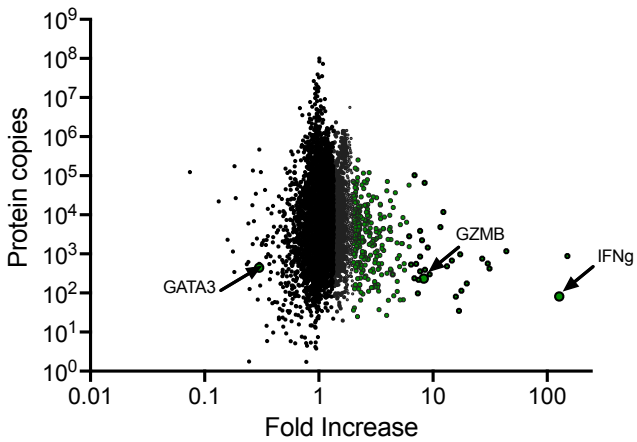

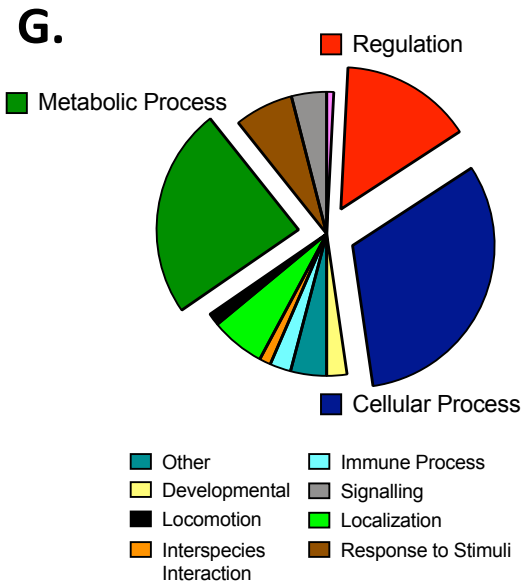

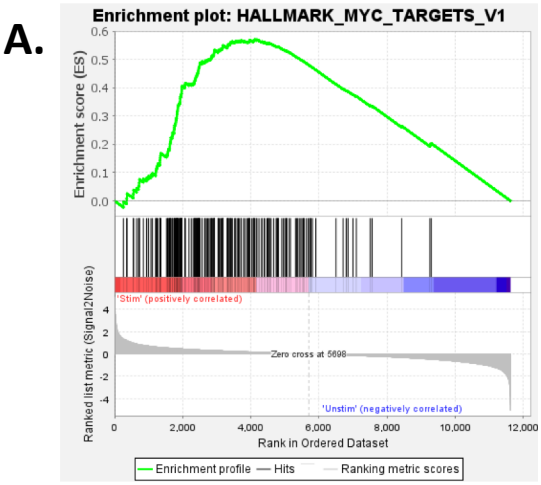

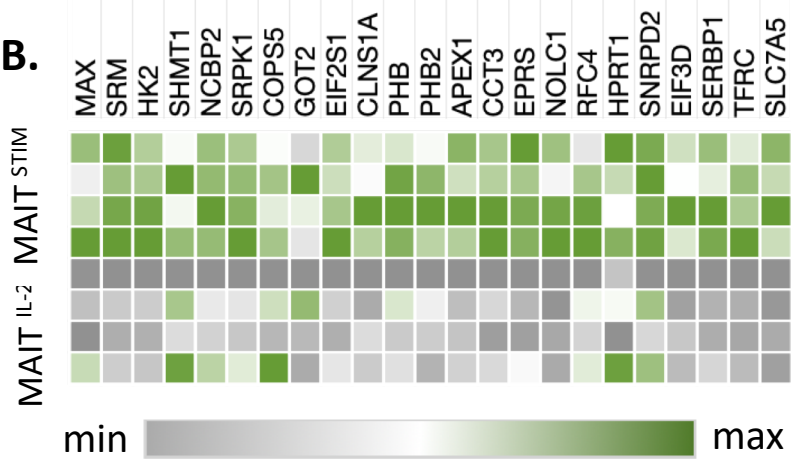

Lamichhane et al, 2019

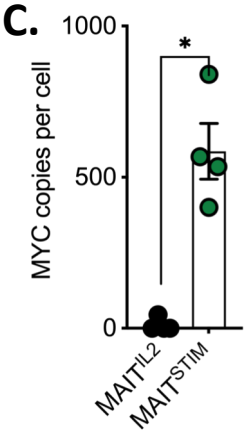

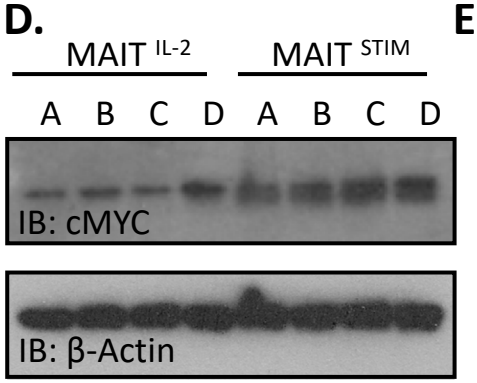

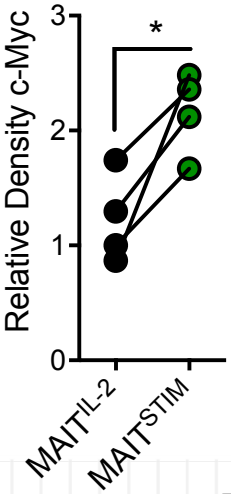

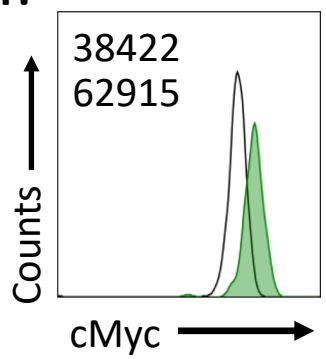

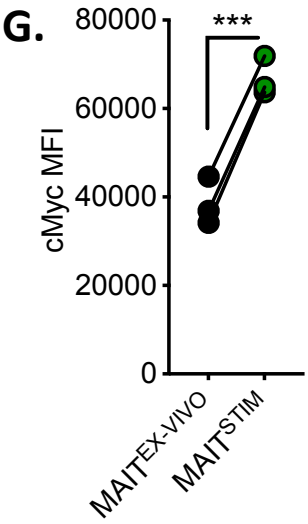

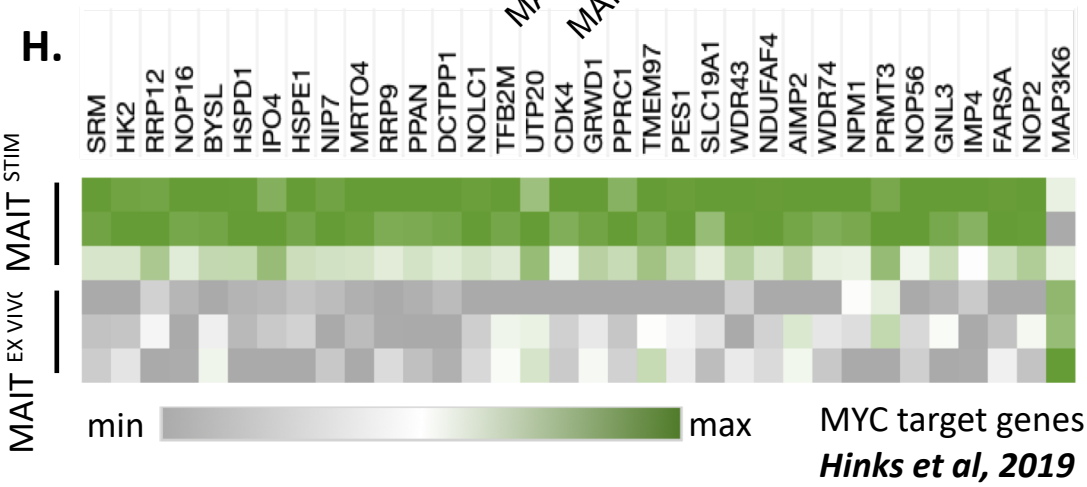

Hinks et al, 2019

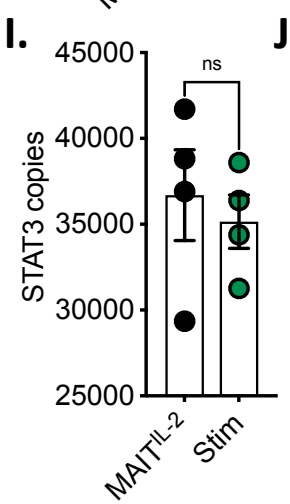

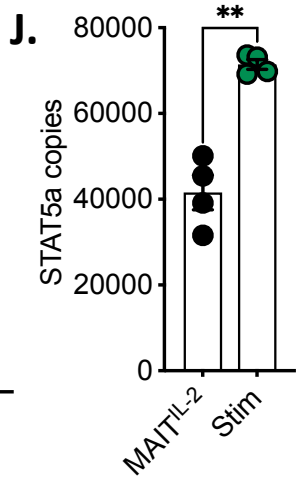

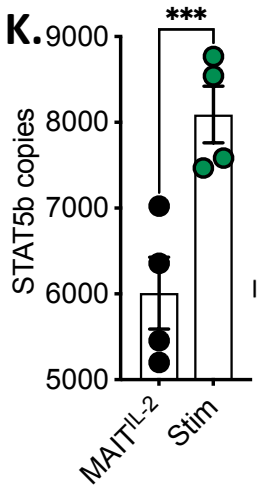

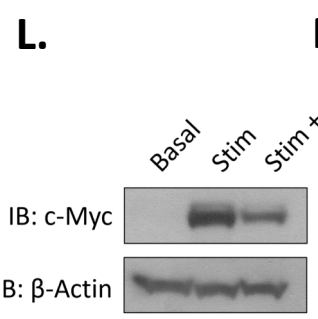

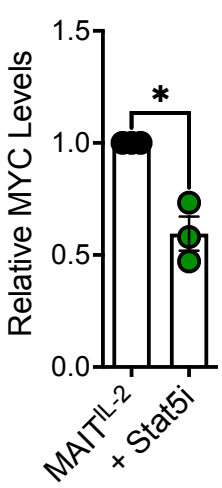

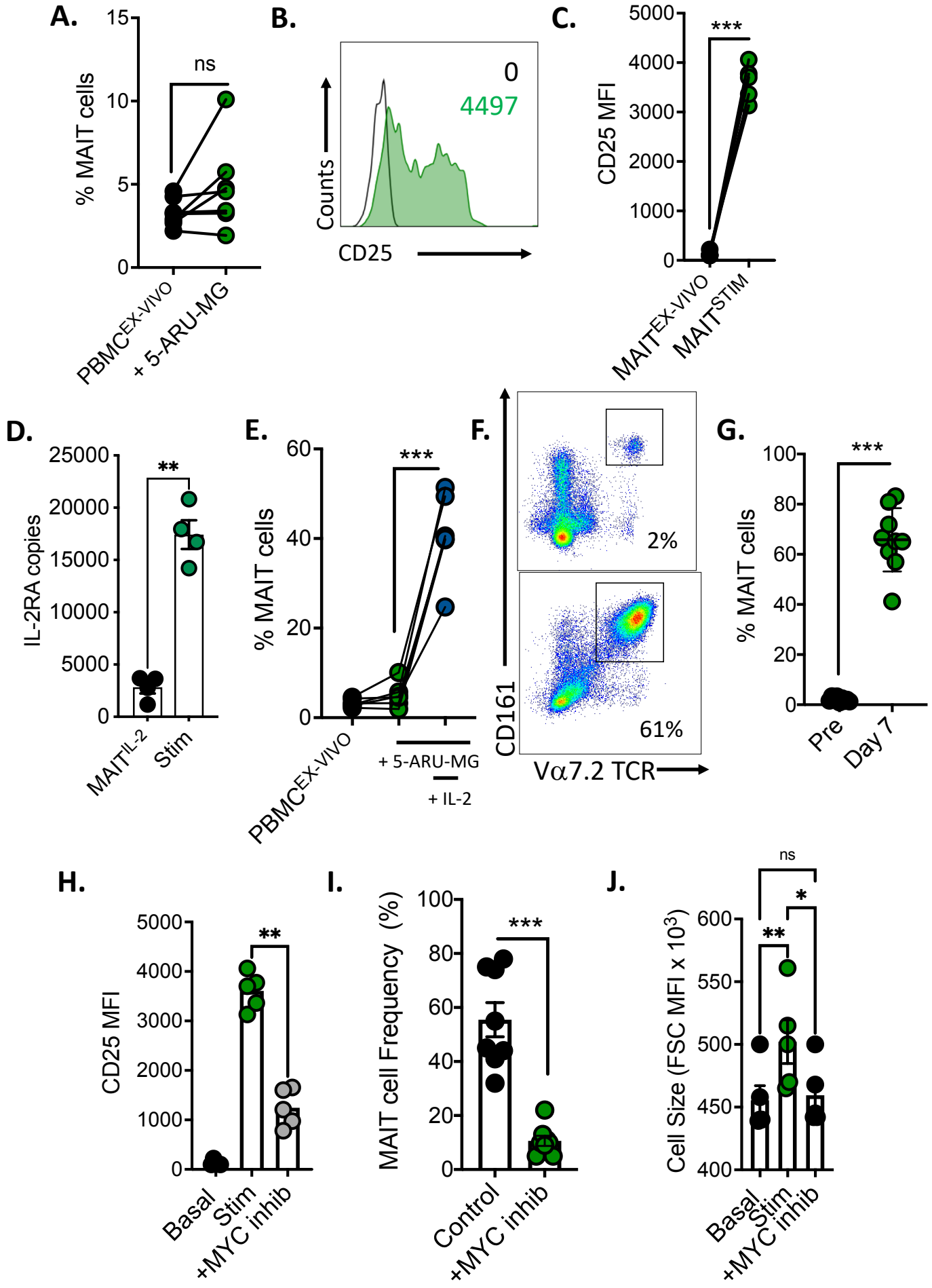
A.
% MAIT cells
ns
PBMC EX-VIVO
+ 5-ARU-MG
B.
0
4497
Counts
CD25
C.
CD25 MFI
***
MAIT EX-VIVO
MAIT STIM
D.
IL-2RA copies
**
MAIT IL-2
Stim
E.
% MAIT cells
***
PBMC EX-VIVO
+ 5-ARU-MG
+ IL-2
F.
2%
61%
CD161
Vα7.2 TCR
G.
% MAIT cells
***
Pre
Day 7
H.
CD25 MFI
**
Basal
Stim
+MYC inhib
I.
MAIT cell Frequency (%)
***
Control
+MYC inhib
J.
Cell Size (FSC MFI x 10³)
ns
*
**
Basal
Stim
+MYC inhib

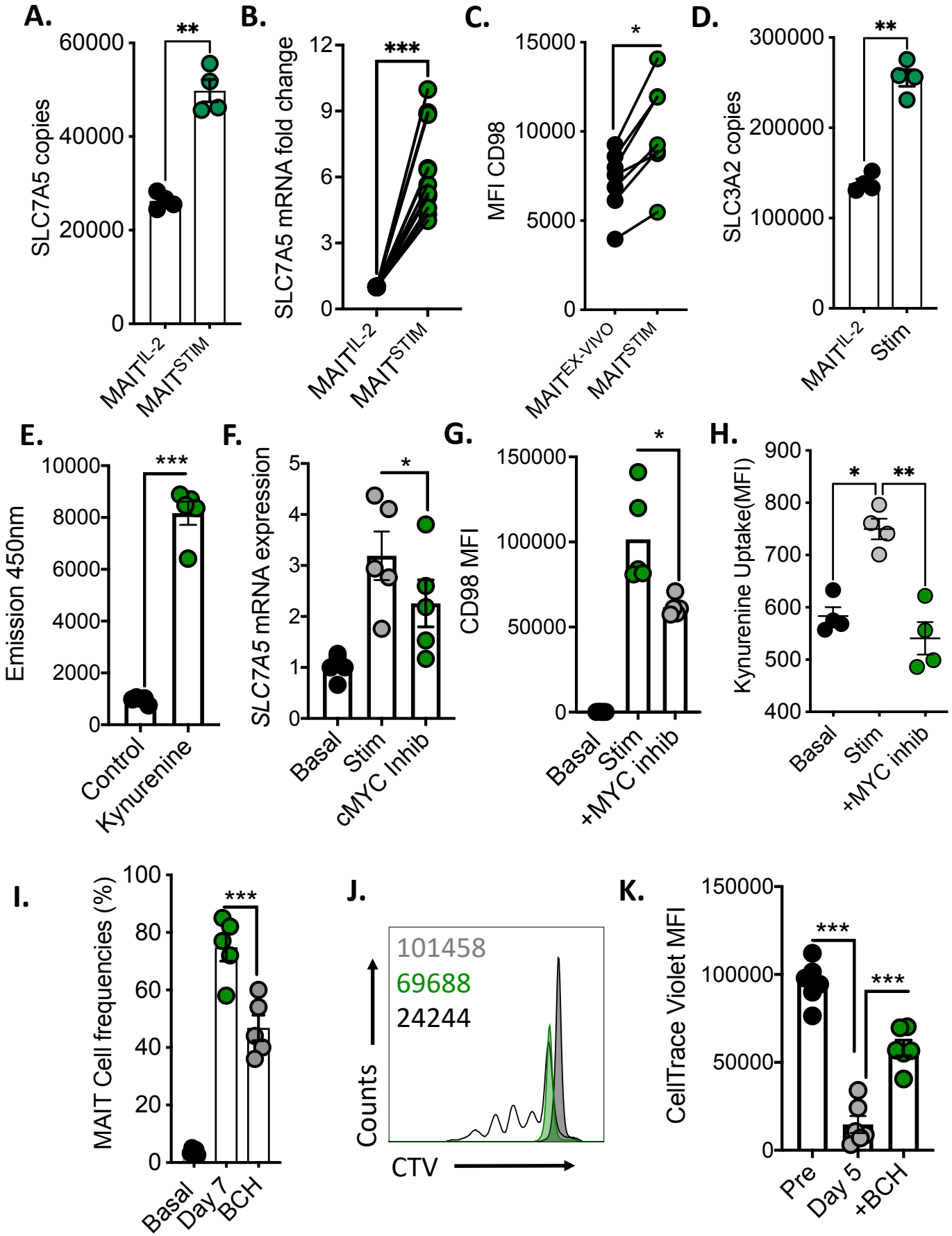
A.
SLC7A5 copies
60000
40000
20000
0
**
MAIT^IL-2
MAIT^STIM
B.
SLC7A5 mRNA fold change
12
9
6
3
0
***
MAIT^IL-2
MAIT^STIM
C.
MFI CD98
15000
10000
5000
0
*
MAIT^EX-VIVO
MAIT^STIM
D.
SLC3A2 copies
300000
200000
100000
0
**
MAIT^IL-2
Stim
E.
Emission 450nm
10000
8000
6000
4000
2000
0
***
Control
Kynurenine
F.
SLC7A5 mRNA expression
5
4
3
2
1
0
*
Basal
Stim
cMYC Inhib
G.
CD98 MFI
150000
100000
50000
0
*
Basal
Stim
+MYC inhib
H.
Kynurenine Uptake(MFI)
900
800
700
600
500
400
*
**
Basal
Stim
+MYC inhib
I.
MAIT Cell frequencies (%)
100
80
60
40
20
0
***
Basal
Day 7
BCH
J.
101458
69688
24244
Counts
CTV
K.
CellTrace Violet MFI
150000
100000
50000
0
***
***
Pre
Day 5
+BCH

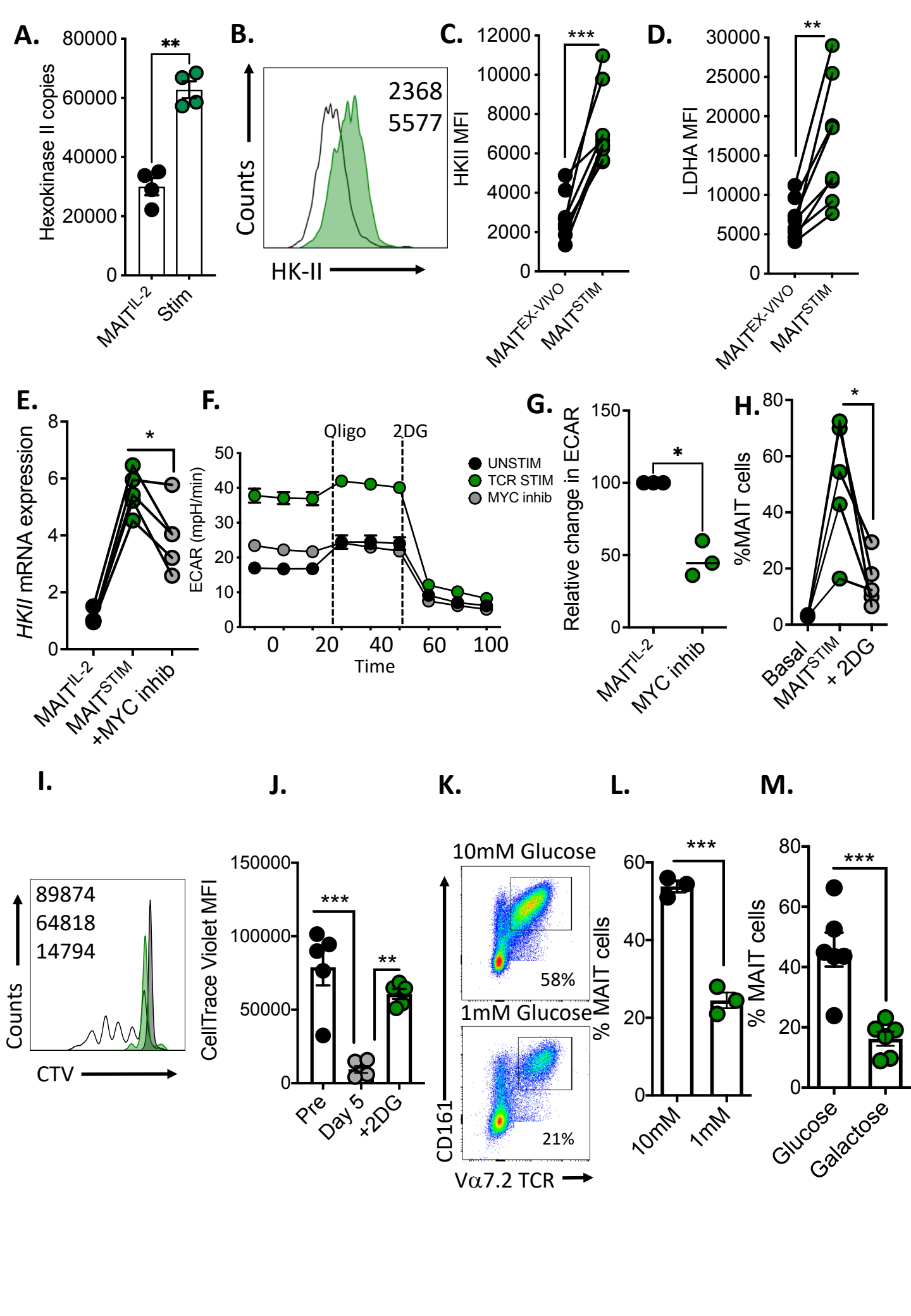
A.
Hexokinase II copies
80000
60000
40000
20000
0
**
MAIT IL-2
Stim
B.
Counts
2368
5577
HK-II
C.
HKII MFI
12000
10000
8000
6000
4000
2000
0
***
MAIT EX-VIVO
MAIT STIM
D.
LDHA MFI
30000
25000
20000
15000
10000
5000
0
**
MAIT EX-VIVO
MAIT STIM
E.
HKII mRNA expression
8
6
4
2
0
*
MAIT IL-2
MAIT STIM
+MYC inhib
F.
Oligo
2DG
ECAR (mpH/min)
50
40
30
20
10
0
0
20
40
60
100
Time
UNSTIM
TCR STIM
MYC inhib
G.
Relative change in ECAR
150
100
50
0
*
MAIT IL-2
MYC inhib
H.
%MAIT cells
80
60
40
20
0
*
Basal
MAIT STIM
+ 2DG
I.
Counts
89874
64818
14794
CTV
J.
CellTrace Violet MFI
150000
100000
50000
0
***
**
Pre
Day 5
+2DG
K.
10mM Glucose
58%
1mM Glucose
21%
CD161
Vα7.2 TCR
% MAIT cells
L.
60
40
20
0
***
10mM
1mM
M.
% MAIT cells
80
60
40
20
0
***
Glucose
Galactose

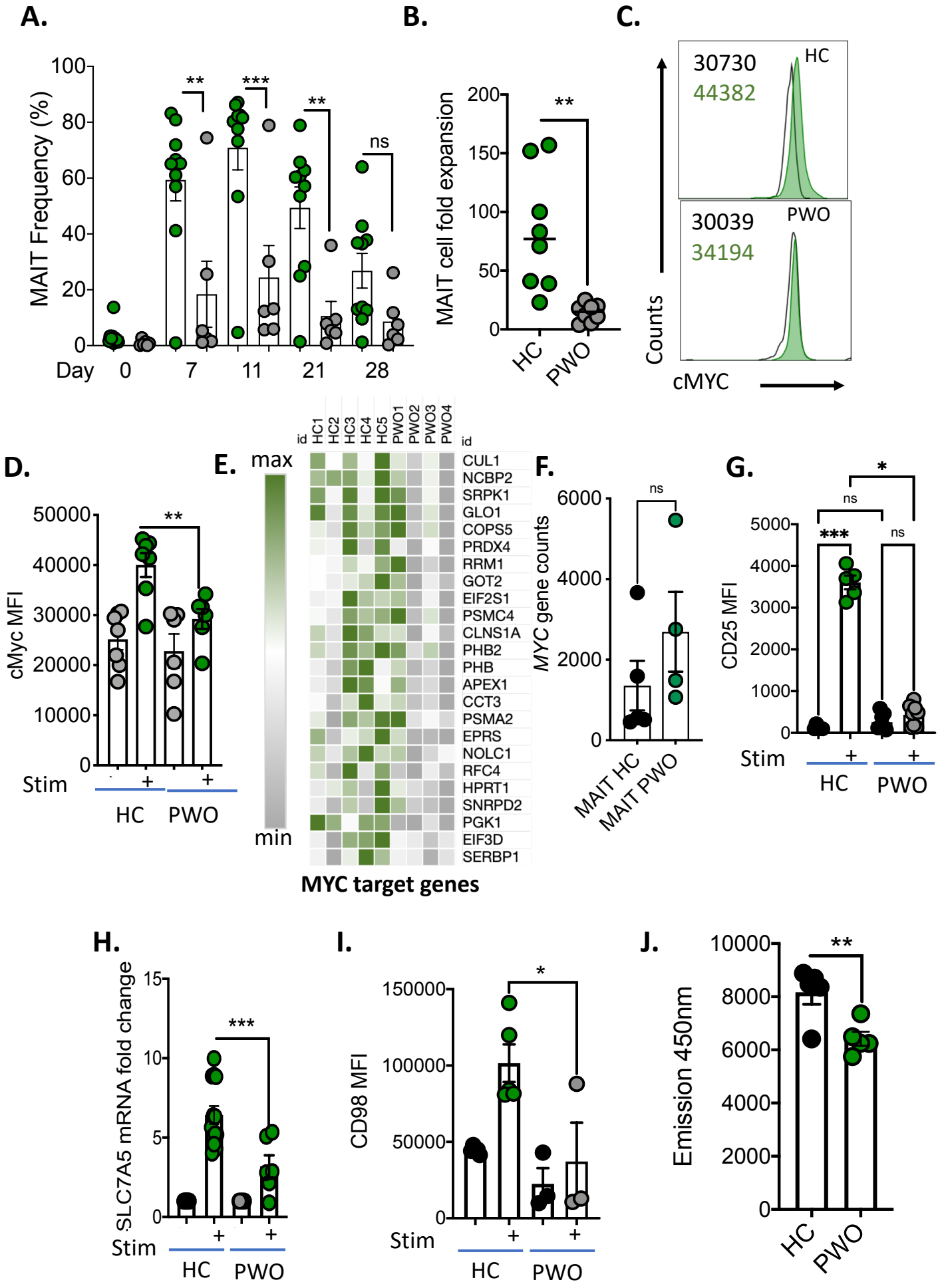
A.
MAIT Frequency (%)
Day 0 7 11 21 28
**
***
**
ns
B.
MAIT cell fold expansion
HC
PWO
**
C.
30730
44382
HC
30039
34194
PWO
Counts
cMYC
D.
cMyc MFI
Stim
HC
PWO
**
E.
max
min
id
HC1 HC2 HC3 HC4 HC5 PWO1 PWO2 PWO3 PWO4
CUL1
NCBP2
SRPK1
GLO1
COPS5
PRDX4
RRM1
GOT2
EIF2S1
PSMC4
CLNS1A
PHB2
PHB
APEX1
CCT3
PSMA2
EPRS
NOLC1
RFC4
HPRT1
SNRPD2
PGK1
EIF3D
SERBP1
MYC target genes
F.
MYC gene counts
MAIT HC
MAIT PWO
ns
G.
CD25 MFI
Stim
HC
PWO
*
ns
***
ns
H.
SLC7A5 mRNA fold change
Stim
HC
PWO
***
I.
CD98 MFI
Stim
HC
PWO
*
J.
Emission 450nm
HC
PWO
**